Estuarine and Coastal Marine Science (1978) 7, 347–359

Turbidity Maxima in Partially Mixed Estuaries: A Two-Dimensional Numerical Model

John F. Festa and Donald V. Hansen

National Oceanic and Atmospheric Administration, Atlantic Oceanographic and Meteorological Laboratories, 15 Rickenbacker Causeway, Virginia Key, Miami, Florida 33149, U.S.A.

Received 17 June 1977

Keywords: numerical model; suspended sediments; estuarine circulation; partially mixed estuary; gravitational circulation; sediment transport; turbidity; settling rates

A steady-state numerical model has been developed to help explain the presence of the turbidity maximum in partially mixed estuaries. The model supports the hypothesis that estuarine dynamics are primarly responsible for its occurrence.

The magnitude and location of the turbidity maximum is shown to depend upon the settling velocity (particle size) of the sediment, the amount of sediment introduced at both the ocean and river source, and the strength of the estuarine circulation. This phenomenon is not simply related to the river input of sediments, since results show the existence of a turbidity maximum for a sediment source which is predominately oceanic. Sediment flux stream functions show the presence of a closed cell when a turbidity maximum exists.

Introduction

Turbidity maxima, regions in which the concentration of suspended sediments is greater than in either the landward or seaward source waters, have been observed in many estuaries. They are observed typically near the landward limit of salt intrusion into the estuary. The most popular, and intuitively appealing, mechanism proposed for the occurrence of the maxima is that they are produced by the estuarine circulation pattern which is convergent in the lower portion of the water column. Postma (1967) gives a particularly lucid account of this hypothesized mechanism. He indicates that the magnitude of the maxima depends upon the amount of suspended material at both the river and ocean source, the settling velocity of the sediment, and the strength of the estuarine circulation. Three other processes, flocculation (Lüneburg, 1939; Ippen, 1966; and others) and deflocculation (Nelson, 1959) regulated by salinity variation, and local resuspension by tidal currents or waves (Schubel, 1968*a*; and others) have been offered as alternative or contributing mechanisms.

The logical connection between estuarine circulation and formation of the turbidity maximum has not been rigorously demonstrated. The purpose of this paper is to investigate this relationship by means of a dynamically consistent model of circulation and suspended sediment transport. The description by Postma (1967) is found to be correct in all of its major features, and further comments are made on some consequences of the process.

0302–3524/78/100347+13 $02.00/0

Circulation model

A detailed and accurate description of the circulation field is critical to any model simulating the transport of a substance within an estuary. Velocity distributions obtained from a circulation model for partially mixed estuaries (Festa & Hansen, 1976) satisfy such requirements. The circulation model is briefly described below.

The problem considered is that of a steady-state, two-dimensional, laterally homogeneous estuary. The coordinate system is Cartesian in x and z, where x increases toward the river, and z is positive upward. A linear equation of state, $\rho = \rho_0(1+\beta S)$, is assumed, and the Boussinesq approximation (Spiegel & Veronis, 1960) is employed.

The horizontal and vertical momentum balances, continuity of flow, and conservation of salinity are:

$$u_t + uu_x + wu_z = -\rho_0^{-1}P_x + (A_h u_x)_x + (A_v u_z)_z, \tag{1a}$$

$$w_t + uw_x + ww_z = -\rho_0^{-1}P_z + (A_h w_x)_x + (A_v w_z)_z - \beta g S, \tag{1b}$$

$$u_x + w_z = 0, \tag{1c}$$

$$S_t + uS_x + wS_z = (K_h S_x)_x + (K_v S_z)_z, \tag{1d}$$

where u and w are the horizontal and vertical components of velocity respectively, P is the hydrostatically reduced pressure, S is the salinity field, β is the coefficient of 'salt contraction', ρ_0 is the density of fresh water, A_h, A_v, and K_h, K_v are the horizontal and vertical exchange coefficients of momentum and salt, respectively, and g is the gravitational acceleration.

Although tidal fluctuations have been averaged out the tides are considered to be the primary source of energy for turbulent mixing. For simplicity, the exchange coefficients, a measure of the tidal strength, are chosen to be constant, as are the depth and width of the estuary.

The equations (1a), (1b), and (1c) are used to write a vorticity equation in terms of a stream function. The vorticity and salt equation, (1d), are non-dimensionalized and solved numerically for various river flow conditions, assuming reasonable values for the exchange (diffusion) coefficients. The model describes the transition from river to estuarine dynamics and its variations with river inflow. A detailed description of the model assumptions, boundary conditions, and finite difference techniques have been presented by Festa & Hansen (1976).

Suspended sediment model

The suspended sediment model is consistent with the circulation model, in that the same exchange coefficients are used for sediments as for salinity, and the advection is by currents derived from the circulation model. Consideration is limited to conditions in which sediment concentration has a negligible effect on water density.

Governing equation

The equation governing the distribution of suspended sediment in the estuary is:

$$C'_t + uC'_x + (w+W)C'_z = K_h C'_{xx} + K_v C'_{zz}, \tag{2}$$

where C' is the concentration of suspended sediment, u and w are the circulation velocities, K_h and K_v are the exchange coefficients as previously described, and W represents the

settling velocity of the sediment. W is considered to be constant; therefore, specifying W is roughly equivalent to specifying the grain size of the sediment to be modeled.

The concentration, C', is normalized by $C' = C_r C$, where C_r represents the bottom concentration at the river boundary. Equation (2) is then written in terms of a stream function, ψ:

$$C_t = -\mathcal{J}(\psi, C) + K_h C_{xx} + K_v C_{zz} - WC_z, \tag{3}$$

where

$$u = -\psi_z \text{ and } w = \psi_x; \tag{4}$$

$\mathcal{J}$ is the Jacobian.

Boundary conditions

The computational length and depth of the estuary are given by L and H respectively. Zero total vertical flux of sediment is required at both the bottom and top boundaries (the vertical flow, w, is zero at these boundaries):

$$WC - K_v C_z = 0 \text{ at } z = 0, H. \tag{5}$$

These conditions require zero net deposition or erosion of bottom sediments and sediment conservation at the upper surface.

Sediment sources are maintained at the bottom at the seaward and river ends:

$$\begin{aligned} C = R_c^{-1} = C_0/C_r &\text{ at } (x, z) = (0, 0), \\ C = 1 &\text{ at } (x, z) = (L, 0), \end{aligned} \tag{6}$$

where C_0 and C_r are the sediment concentrations at the ocean and river respectively; R_c is the river-to-ocean source concentration ratio.

An exponential profile is maintained at the river end:

$$C(z) = e^{\lambda z/H} \text{ at } x = L, \tag{7}$$

where $\lambda = WH/K_v$. This is the appropriate analytical solution at the river end, where the horizontal advective and diffusive sediment flux divergence is zero.

The horizontal diffusive flux of sediment, $K_h C_x$, is required to be unspecified but horizontally non-divergent at the open seaward boundary. This is in agreement with the boundary condition used for modeling the estuarine dynamics (Festa & Hansen, 1976).

Numerical formulation and procedures

The spacing of the finite difference grid is chosen to be uniform in x, z and t such that

$$\begin{aligned} x_i &= i\Delta x, \; i = 0, 1, \ldots . I \\ z_j &= j\Delta z, \; j = 0, 1, \ldots . \mathcal{J} \\ t^n &= n\Delta t, \; n = 0, 1, \ldots , \end{aligned} \tag{8}$$

where $\Delta x = L/I$, $\Delta z = H/\mathcal{J}$ and Δt is the time step. Diffusion is approximated by the time-centered scheme of DuFort-Frankel (1953) and advection by the conservative form of the Jacobian (Arakawa, 1966) for which both C and C^2 are conserved. The resulting finite difference analog to (3) is:

$$\begin{aligned} (C^{n+1}_{ij} - C^{n-1}_{ij})/2\Delta t = &-\mathcal{J}^n(\psi, C)/4\Delta x \Delta z + K_h/\Delta x^2 (C^n_{i+1,j} + C^n_{i-1,j} - C^{n+1}_{ij} - C^{n-1}_{ij}) \\ &+ K_v/\Delta z^2 (C^n_{ij+1} + C^n_{ij-1} - C^{n+1}_{ij} - C^{n-1}_{ij}) \\ &- W/2\Delta z (C^n_{ij+1} - C^n_{ij-1}). \end{aligned} \tag{9}$$

The numerical formulation of the bottom and top boundary conditions presented a major difficulty in the analysis. Conservative forms (Fix, 1975) of these boundary conditions, (6), are given by:

$$W(C_{i0}^{n+1}+C_{i1}^{n-1})/2 = K_v/\Delta z(C_{i1}^{n+1}-C_{i0}^{n+1}) \text{ at } z = 0,$$
$$W(C_{iJ}^{n+1}+C^{n-1}_{iJ-1})/2 = K_v/\Delta z(C_{iJ}^{n+1}-C^{n+1}_{iJ-1}) \text{ at } z = H. \quad (10)$$

New boundary values, C_{i0}^{n+1} and C_{iJ}^{n+1}, are, therefore, calculated based on the computed interior points next to the boundary. While this is the conservative formulation of the flux condition, the accuracy of the solutions, nevertheless, depends critically upon the grid spacing and the magnitude of λ (see Fix, 1975, for a complete analysis). A 33×33 finite difference grid is used for all calculations.

The procedure followed to obtain the steady-state suspended sediment distribution is:

(1) Compute the steady-state circulation field for the desired mixing coefficients and river flow.

(2) Place this information, via the stream function, into the sediment model.

(3) Specify the settling velocity, W, and initialize the sediment distribution as:

$$C(x, z) = e^{\lambda z/H}\{R_c^{-1}+(1-R_c^{-1})x/L\}. \quad (11)$$

(4) Start the calculation and continue until the sediment field has converged to a steady state.

(5) Check the suspended sediment distribution for mass conservation.

Model calculations

This model has been developed to help understand the basic processes which influence the distribution of suspended sediments in partially mixed estuaries. As no attempt has been made to model any particular estuary, the reader is cautioned about applying these results quantitatively: qualitatively, the results presented in the following sections will behave similarly for a range of estuarine dynamics; quantitatively they will of course depend critically on the choice of mixing coefficients and river discharge.

Estuarine circulation

The circulation model was run for a depth-averaged river flow, U_f, of 2 cm s^{-1}, depth, H, of 10 m, and length, L, of 120 km. A horizontal salinity difference, ΔS_h, of 30‰ is maintained between the seaward and river boundaries, and the mixing coefficients (in cm^2 s^{-1}) are: $K_v = 1$, $A_v = 10$, $K_h = 10^6$, and $A_h = 10^7$. These parameters are characteristic values typical of coastal plain estuaries (Dyer, 1973; Officer, 1976). As used in the model, they result in an estuary in which the circulation has a seaward transport of 2·4 river discharge volumes per unit width and a landward transport of 1·4.

Salinity and stream function contours [Figures 1(a) and (b)] show a stratified intrusion of salt into the estuary, and the typical estuarine pattern of seaward flow of near surface water and landward flow of deeper water. Contours of the velocity distributions are also presented [Figures 1(c) and (d)]. Maximum horizontal surface velocities exceed 16 cm s^{-1}, while the maximum landward velocities exceed 8 cm s^{-1} at the seaward boundary. Both seaward and landward velocities attenuate landward. The stagnation point (null zone), the location of zero horizontal velocity near the bottom, is at 60 km. The vertical component of flow, w, [Figure 1(d)] is of considerable interest, since sediment-particle settling behavior will depend critically on its magnitude and distribution. The maximum vertical velocity,

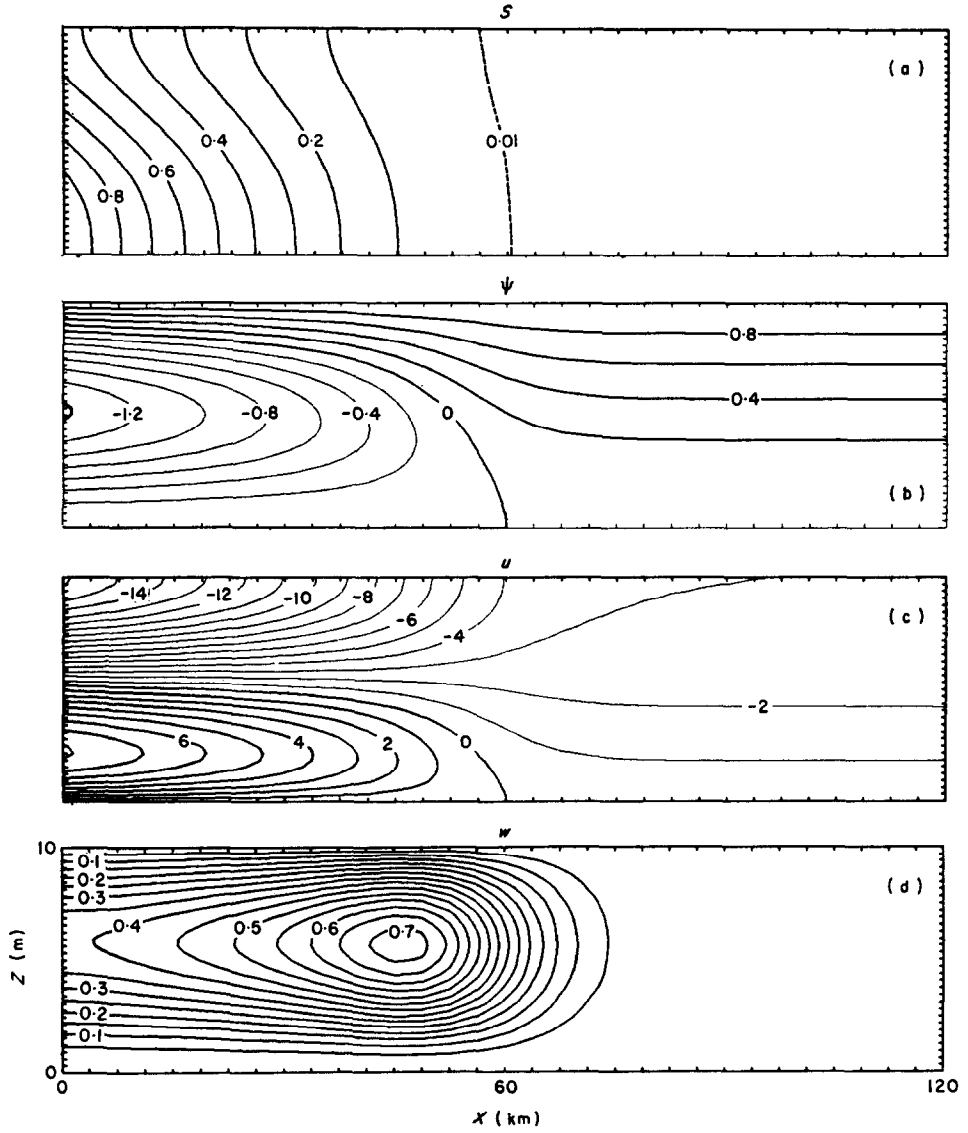

Figure 1. Salinity (a), stream function (b), horizontal velocity (c), and vertical velocity (d) fields for the case of $U_f = 2$ cm s^{-1}, $H = 10$ m and $L = 120$ km. Salinity is scaled by $\Delta S_h = 30‰$, stream function by 2×10^3 cm^2 s^{-1} and w by 10^{-3}. Velocity fields are contoured in cm s^{-1}.

approximately 7×10^{-4} cm s^{-1}, is located some 10 km seaward of the stagnation point. Attenuation of vertical velocity is greatest just landward of the maximum. At any given x, w reaches a maximum near mid-depth.

The effect of varying river flow is discussed in detail in the circulation paper (Festa & Hansen, 1976); a summary of these results is presented here.

As freshwater discharge is increased, there is an increase in both stratification and strength of the estuarine circulation. Increasing river discharge results in an increase in the magnitude of the vertical velocity as well as a seaward displacement of its spatial maximum (Figure 2).

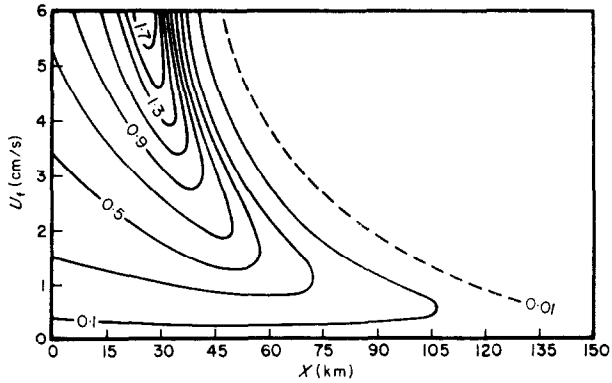

Figure 2. Vertical velocity contours at mid-depth as function of river discharge, U_f. Vertical velocity contours are scaled by 10^{-3} cm s^{-1} with a contour interval of 0·2.

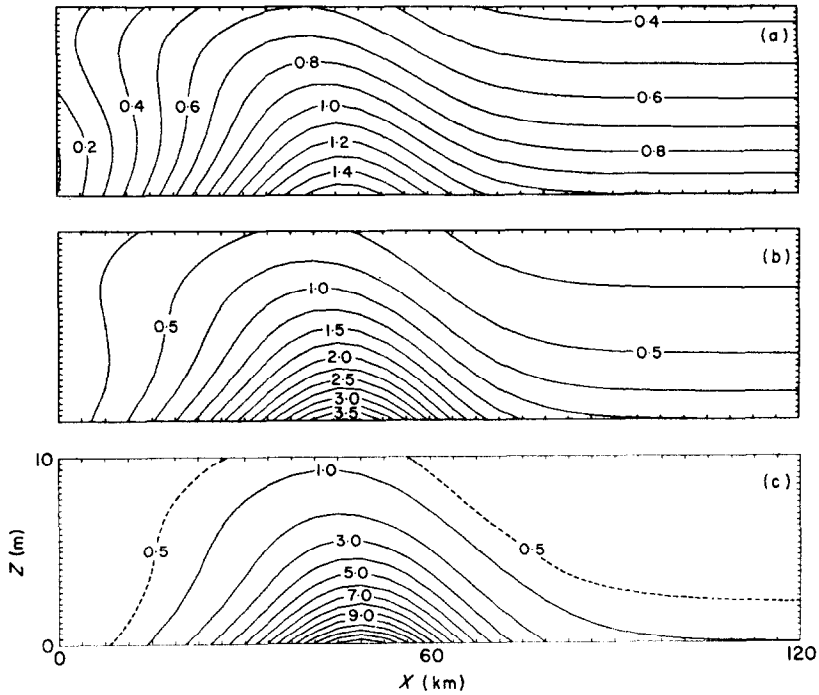

Figure 3. Suspended sediment distributions for particle settling velocities, W, of -1×10^{-3} cm s^{-1} (a), -2×10^{-3} cm s^{-1} (b), and -3×10^{-3} cm s^{-1} (c). The river-to-ocean source ratio, $R_c = 10$ for each case.

Decreasing river discharge allows salt to intrude farther up the estuary and also results in greater landward migration of the stagnation point. The effects of river discharge on the distribution of suspended sediments will be briefly discussed in a later section.

Suspended sediment distribution

Influence of settling velocity. Steady-state suspended sediment distributions are obtained for settling velocities, W, ranging from 0 to -3×10^{-3} cm s^{-1}, for the estuarine circulation associated with $U_f = 2$ cm s^{-1}. These settling velocities correspond to Stokes velocities

associated with sediment particle diameters of 1 to 6 μm (clay to very fine silt) for particle densities of 2·65 gm cm^{-3}. This size distribution is commonly observed in partially mixed estuaries (Schubel, 1969; Meade, 1972; Nichols, 1974; Conomos & Peterson, 1977). The concentration of sediment at the river source, for this simulation, is considered to be 10 times the ocean source ($R_c = 10$), a condition similar to estuaries studied by Postma (1967) and Allen *et al.* (1974).

Contours of the suspended sediment distribution (Figure 3) show the presence of a concentration, or turbidity, maximum which is located approximately 45 km from the seaward boundary. This corresponds closely to the location of the maximum vertical velocity associated with the estuarine circulation [Figure 1(d)]. At settling velocities less than -5×10^{-4} cm s^{-1}, but non-zero, the concentration maximum decreases substantially, and its location approaches the stagnation point. Zero settling velocity produces pure advection and gradient diffusion so no concentration maximum occurs; the solutions are nearly the inverse of salinity, with small differences associated with the non-zero ocean source.

Dependence of the magnitude of the maximum on settling velocity (and implicitly on particle size) is better exemplified in Figure 4. A small concentration maximum is present for $W < -5 \times 10^{-4}$ cm s^{-1}; however, for $W > -5 \times 10^{-4}$ cm s^{-1} there is a substantial

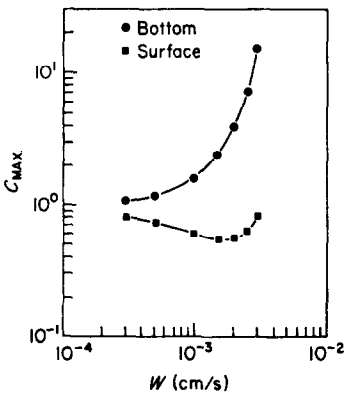

Figure 4. Magnitude of the concentration maximum as a function of particle settling velocity, W, at the surface and bottom boundary.

increase in its magnitude. Results are not presented for settling velocities beyond -3×10^{-3} cm s^{-1}, because the choice of mixing coefficients and the vertical resolution used gives erroneous solutions when W exceeds this value. Furthermore, the bottom boundary condition which requires total resuspension is not appropriate for particles having large settling velocities relative to the mixing conditions within an estuary.

Influence of sediment sources

The effect of the relative strengths of river and ocean sources of sediment was examined by varying the river-to-ocean source concentration ratio, R_c, from 0·01 to 100. Contours of the suspended sediment for two settling velocities, $W = -1$ and -2 ($\times 10^{-3}$ cm s^{-1}), and different values of R_c (Figures 5 and 6) clearly show the dependence of both magnitude and location of turbidity maxima on R_c. Increasing the ocean source concentration

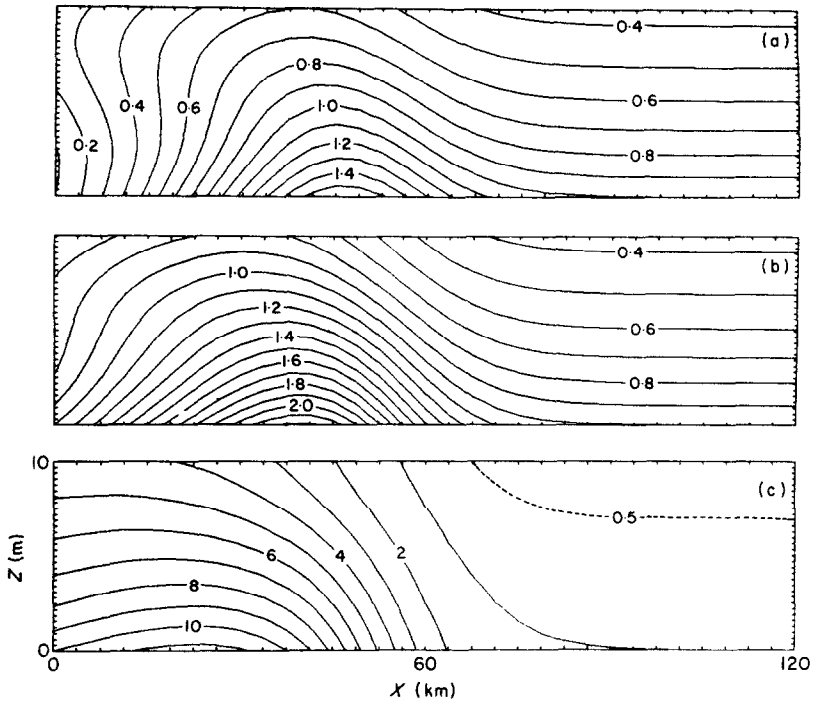

Figure 5. Suspended sediment distributions for a river-to-ocean source concentration ratio, R_c, of 10 (a), 1 (b), and 0·1 (c). Particle settling velocity, W, is -1×10^{-3} cm s^{-1}.

results in an increase in concentration values throughout the estuary. The turbidity maximum shifts seaward as R_c decreases; however, this shift is slight when $W = -2 \times 10^{-3}$ cm s^{-1}.

The magnitude of the concentration maximum at the bottom boundary, is presented as a function of settling velocity for $R_c = 10$ and 1 (Figure 7). Concentrations become higher as the ocean source becomes equivalent to the river; however, the general behavior is similar for each source ratio. This is also seen (Figure 8) where the source ratio for two settling velocities has been varied over a wider range. When the ocean contributes substantially to the estuarine suspended sediment budget, $R_c < 1$, the water column storage of sediments is not simply related to the river input. For $R_c < 1$, normalizing concentrations by the ocean boundary source is more logical than scaling by the river source. The result of this alternative normalization is also shown (Figure 8). The combination of these normalized curves has a maximum at $R_c = 1$ because the mass sediment flux into the estuary is a maximum at $R_c = 1$. Results of using still a third kind of normalization, the sum of the bottom river and ocean source concentrations as a measure of the total sediment source strength, is also presented (Figure 8). For the estuarine circulation parameters used, and a sediment characterized by a settling velocity of -2×10^{-3} cm s^{-1}, the turbidity maximum is approximately four times the total source concentration, and it is independent of how the source is distributed between the river and the ocean. For a smaller settling velocity (-1×10^{-3} cm s^{-1}) however, the situation is somewhat different. The turbidity maximum then varies from 1·5 times the total source concentration when the source is in the river to less than 1·1 times the source concentration when the source is in the ocean.

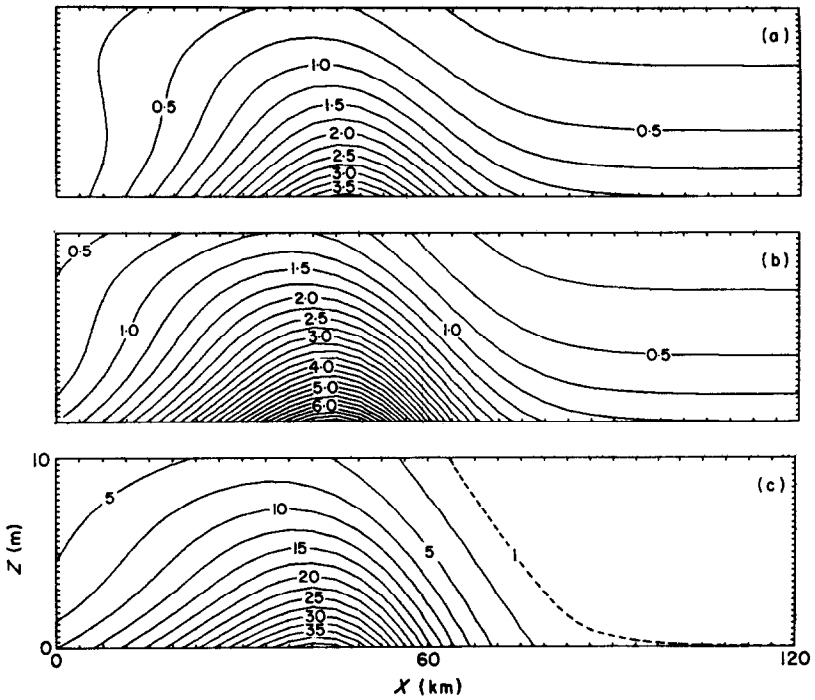

Figure 6. Suspended sediment distributions for river-to-ocean source concentration ratio, R_c, of 10 (a), 1 (b), and 0·1 (c). Particle settling velocity, W, is -2×10^{-3} cm s^{-1}.

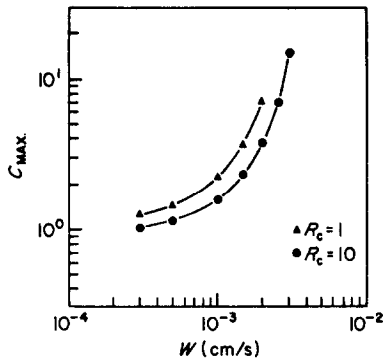

Figure 7. Magnitude of the concentration maximum as a function of particle settling velocity, W, for two river-to-ocean source concentration ratios, R_c.

Sediment flux stream functions

The calculated advective and diffusive fluxes of suspended sediment are used to evaluate[a] a suspended sediment stream function, φ, defined by:

$$uC-K_hC_x = -\varphi_z; \quad (w+W)C-K_vC_z = \varphi_x. \tag{12}$$

[a]This evaluation is readily made by solution of the Poisson equation $\nabla^2\varphi = -\mathbf{k}\cdot\nabla\times\mathbf{F}_s$, where $\mathbf{F}_s$ is the local sediment flux vector, and φ is prescribed around the boundaries.

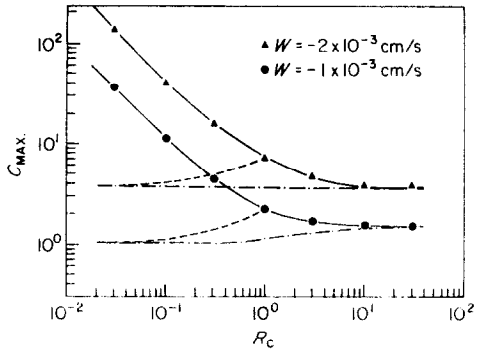

Figure 8. Magnitude of the concentration maximum as a function river-to-ocean source concentration ratio, R_c, for two particle settling velocities, W. Concentrations have been normalized by the river source ————, ocean source – – – –, and the sum of the river and ocean sources · · · ·.

The function φ is analogous to the stream function [Figure 1(b)], but applies to the mass flux distribution of suspended sediment. Typical flux stream function patterns are presented (Figure 9). Contours for concentrations calculated for zero settling velocities and sources located either solely at the ocean or at the river have also been included. These are applicable to the flux of salt or to a dissolved constituent of the river water respectively as well as the limiting case of sediment of negligible settling velocity from the respective sources. It may be noticed that when river and ocean concentrations of such a substance are equal, there are no gradients, and the flux stream function [Figure 9(b)] is equivalent to the flow stream function [Figure 1(b)].

Perhaps the most interesting feature is the existence of closed sediment circulation cells, even for a constituent introduced at the river and having zero settling velocity, and even for a constituent introduced at the ocean if its settling velocity is as large as -2×10^{-3} cm s^{-1}. The patterns of the sediment flux stream function provides further insight on the mechanism of the turbidity maximum. In particular, the existence of closed flux contours which indicate downward flux of sediment in the seaward portion of the cell and upward flux in the landward portion, seems to be a necessary, but not a sufficient, condition for the occurrence of a turbidity maximum.

Consider the concentration of a substance introduced at the ocean and having zero particle settling velocity (the tracer property of salinity distributions are representative of this limiting case). It is readily understood from Figure 1(a), where gradient diffusion of salinity is everywhere upward and Figure 1(d), where the vertical flow rate, of order 5×10^{-4} cm s^{-1}, is also upward, why a turbidity maximum and closed sediment flux stream function do not develop. Now consider the distribution of a zero settling velocity substance introduced at the river; this differs from the distribution of salinity only in having the concentration increase toward the river and surface. Here, we find that gradient diffusion will be downward everywhere; this downward diffusion alone, while providing closed flux stream function contorus [Figure 9(a)], is nevertheless insufficient to produce a turbidity maximum.

The sufficient condition for the development of the turbidity maximum is that the downward flux by particle settling in the seaward portion of the estuary must be sufficient to overcome the upward flux by advection and diffusion. This condition is met for the examples of a dominant river sediment source (Figure 3, note the region of downward diffusive flux near the ocean boundary), as well as for the examples of equal source strengths [Figures 5(b)

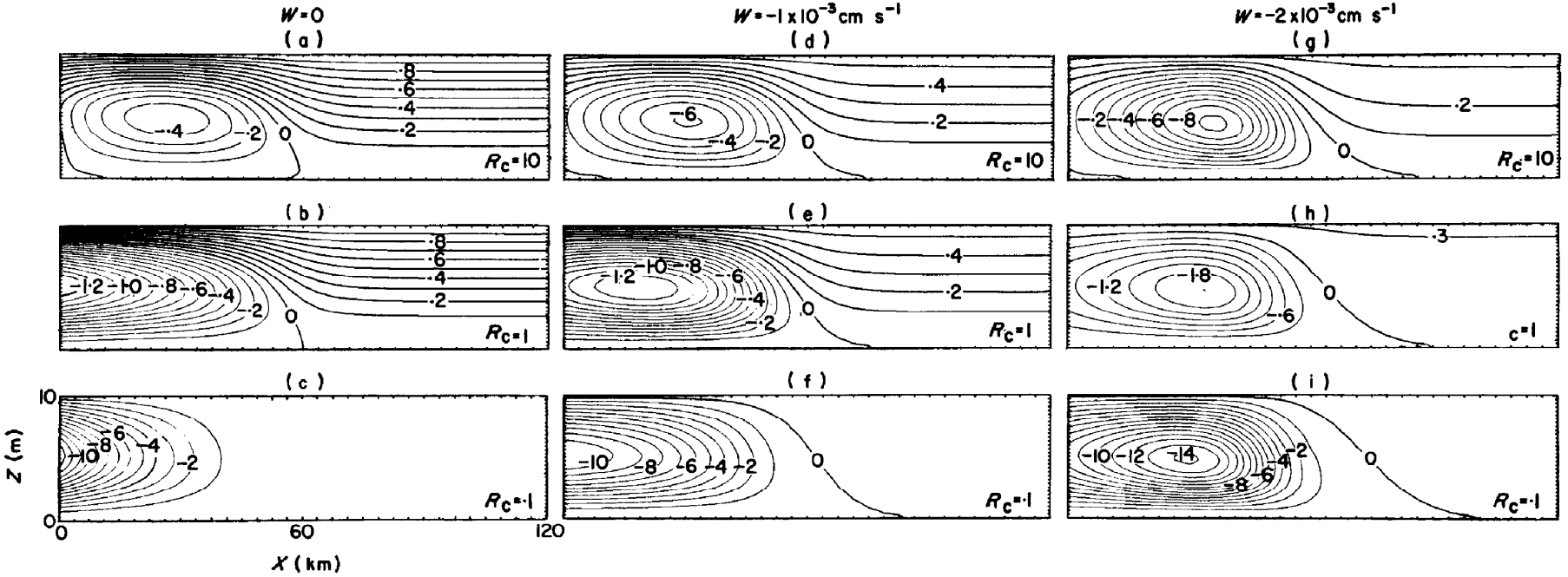

Figure 9. Sediment flux stream function, φ, fields as a function of W and R_c. Contours are scaled by 2×10^{-3}. Panels a, b, and c ($W = 0$), d, e, and f ($W = -1\times10^{-3}\,\mathrm{cm\,s^{-1}}$) and g, h, and i ($W = -2\times10^{-3}\,\mathrm{cm\,s^{-1}}$) are for $R_c = 10$, 1, and 0·1, respectively.

and 6(b)]. However a settling velocity as large as -1×10^{-3} cm s^{-1}, or approximately twice the vertical flow rate, does not produce a significant turbidity maximum from an ocean source [Figure 5(c)], because in that circumstance the diffusive flux in the critical region is too strongly upward to allow recirculation [Figure 9(f)] of sediment. If the settling velocity is doubled in the same situation, upward diffusion [Figure 6(c)] is no longer sufficient to prevent recirculation [Figure 9(i)] and the development of a strong turbidity maximum. It may be noted that due to the rearrangement of the concentration field, the upward diffusive flux is also increased.

Conclusion

The magnitude of the turbidity maximum (relative to the river source concentration) has been shown (Figure 8) to depend upon both the particle settling velocity and the contribution of suspended sediment from an oceanic source. This result agrees with statements by Postma (1967). However, relative to the total source concentration, the magnitude of the maximum depends upon the settling velocity and circulation patterns alone, except at the smallest settling velocities for which the phenomenon is poorly developed.

The lower layer of estuarine flow is one of advective convergence of landward flowing, more oceanic, water and seaward flowing river water toward a stagnation point or null zone on the bottom. Model results indicate that maximum concentration occurs slightly seaward of the stagnation point, where the upward vertical circulation is maximum. Vertical flux of sediment into the seaward flowing upper layer provides for advection of sediment out of the estuary to maintain the equilibrium. Horizontal diffusion is important locally to prevent mass accumulation and to help maintain the sediment distribution. Perhaps the most interesting effect of horizontal diffusion is to displace the near-bottom null zone in suspended sediment transport from that in water transport. This displacement is in the direction of the local flux by gradient diffusion; slightly seaward or landward for a zero settling velocity substance introduced at the river or ocean respectively, and strongly landward for material having a significant settling velocity, the more so as the fraction of materials originating in the ocean increases. This behavior depends in detail upon the specific formulation of the diffusive process in the model, but must apply in principle so long as any form of the gradient diffusion concept is valid.

Effects of varying river flow have also been studied, but the results are not presented in any detail in this paper. Basically, it is found that at higher river flows, the estuarine circulation is stronger, the vertical velocities are larger and, thus, larger settling velocities are required to develop a turbidity maximum. The implication of this finding is that individual estuaries will select from the full range of particles supplied to them, a relatively small range of particles for storage in the water column. This effect was inferred by Postma (1967) and Schubel (1968*a*, *b*). The distribution of particle sizes observed in an estuary cannot be expected to be representative of that supplied to it; however, it must be expected to change in response to dynamic adjustment of the estuary to changes in external variables such as river flow or tidal mixing. The location of the turbidity maximum moves seaward with increasing river discharge as do the stagnation point and salt intrusion. The opposite effect occurs at lower river flows, where smaller settling velocities can produce concentration maxima. Thus, the range in size distribution of suspended sediments varies as the estuarine dynamics change.

Simulation of a range of sediment sizes can be effected by superposition of results for appropriate size distributions. Emphasis is again made that the numerical results relating

to particule size or settling velocity are functionally related to the parameters defining the circulation model, and are to be considered as exemplary rather than definitive.

Real estuaries tend to be strongly depositional environments in which sediments from the ocean and some fraction of sediments from rivers accumulate. In order to focus on the mechanism of the turbidity maximum by setting aside questions of sediment mass flux and retention rates, a somewhat artificial model with equilibrium 'flow thru' has been postulated. Extrapolation of the concepts presented here in the direction of small (down to zero) settling velocity is expected to be valid. Extension of results to higher settling velocities (Figure 4 or 7) becomes progressively less meaningful because complete resuspension of the larger particle sizes especially is unrealistic. The more complete model would be of interest. The principal problem to be solved for its development is a suitable formulation of the bottom boundary condition on sediment deposition and resuspension rates.

Acknowledgements

The progress of this research has benefitted from numerous discussions and criticisms by Drs D. Behringer, W. Lavelle, A. Leetmaa, C. Thacker and R. Young. The authors give special thanks to Drs J. Conomos and D. Peterson for their helpful suggestions, guidance and encouragement during the conception of this work.

References

Allen, G. P., Castaing, P. & Klingebiel, A. 1974 Suspended sediment transport and deposition in the Gironde Estuary and adjacent shelf. *Memoires de l'Intsitute de Geologie du Bassin d'Aquitaine* **7**, 27–36.

Arakawa, A. 1966 Computational design for long-term numerical integration of the equations of fluid motion. Two-dimensional incompressible flow. Part I. *Journal of Computational Physics* **I**, 119–143.

Conomos, T. J. & Peterson, D. H. 1977 Suspended Particle Transport and Circulation in San Francisco Bay: An Overview. In *Estuarine Processes*, Vol. II, Academic Press, New York. pp. 82–97.

Dufort, E. C. & Frankel, S. P. 1953 Stability conditions in the numerical treatment of parabolic differential equations. *Mathematical Tables and Other Aids to Computation* **7**, 135.

Dyer, K. R. 1973 *Estuaries: A Physical Introduction.* Interscience, New York. 140 pp.

Festa, J. F. & Hansen, D. V. 1976 A two dimensional numerical model of estuarine circulation: the effects of altering depth and river discharge. *Estuarine and Coastal Marine Science* **4**, 309–323.

Fix, G. J. 1975 Finite elements and fluid dynamics. Report number 75–1. *Institute for Computer Applications in Science and Engineering.*

Ippen, A. T. 1966 Sedimentation in estuaries. In *Estuary and Coastline Hydrodynamics.* McGraw-Hill, New York. pp. 648–672.

Lüneburg, H. 1939 Hodrochemische untersuchungen in der Elbmundung mittels elektrokolorimeter. *Archiv der Deutschen Seewarte* **59**, pp. 1–27.

Meade, R. H. 1972 Transport and deposition in estuaries. In *Environmental Framework of Coastal Plain Estuaries.* Geological Society of America. Memoir 133, pp. 91–120.

Nelson, B. W. 1959 Transportation of colloidal sediment in the freshwater-marine transition zone. *1st International Oceanographic Congress preprints*, AAAS, (abstract) pp. 640–641.

Nichols, M. M., 1974 Development of the turbidity maximum in the Rappahannock estuary. *Memoires de l'Institut de Geologie du Bassin d'Aquitaine* **7**, 19–25.

Officer, C. B. 1976 *Physical Oceanography of Estuaries (and Associated Coastal Waters).* Interscience, New York. 465 pp.

Postma, H. 1967 Sediment transport and sedimentation in the estuarine environment, In *Estuaries.* AAAS Publication No. 83, pp. 158–179.

Schubel, J. R. 1968*a* The turbidity maximum of the Chesapeake Bay. *Science* **161**, 1013–1015.

Schubel, J. R. 1968*b* Suspended sediment on the Northern Chesapeake Bay. *C.B.I. Technical Report* No. 35. The Johns Hopkins University, 264 pp.

Schubel, J. R. 1969 Size distributions of the suspended particles of the Chesapeake Bay turbidity maxima. *Netherlands Journal of Sea Research* **4**, 283–309.

Spiegel, E. A. & Veronis, G. 1960 On the Boussinesq approximation for a compressible fluid. *Astrophysics Journal* **131**, 442–447.